ELSEVIER

Journal of Photochemistry and Photobiology A: Chemistry 103 (1997) 11–17

Journal of PHOTOCHEMISTRY AND PHOTOBIOLOGY A:CHEMISTRY

Investigation of the collisional behaviour of Ba[6s5d($^3D_{1,2,3}$)] generated following pulsed dye-laser excitation at $\lambda = 553.5$ nm {Ba[6s6p($^1P_1$)] ← Ba[6s^2($^1S_0$)]} by spectroscopic marker methods in the presence of krypton Part II

S. Antrobus, D. Husain *, Jie Lei

Department of Chemistry, University of Cambridge, Lensfield Road, Cambridge CB2 1EW, UK

Received 1 July 1995; accepted 1 October 1996

Abstract

We present a kinetic investigation of Ba[6s5d(^3D_J)], 1.151 eV above the 6s^2($^1S_0$) ground state in the presence of krypton gas following pulsed dye-laser excitation of atomic barium vapour at elevated temperatures at $\lambda = 553.5$ nm {Ba[6s6p($^1P_1$)] ← Ba[6s^2($^1S_0$)]}. The ^3D_J state is neither directly accessible by laser excitation nor is it possible to monitor this state by emission at $\lambda = 1106.9$ nm {Ba[6s5d($^3D_1$)] → Ba[6s^2($^1S_0$)]}. Thus, in the 'long time-domain', Ba(^3D_J) has been monitored by the spectroscopic marker transitions at $\lambda = 791.1$ nm {Ba[6s6p($^3P_1$)] → Ba[6s^2($^1S_0$)]} and $\lambda = 553.5$ nm {Ba[6s6p($^1P_1$)] → Ba[6s^2($^1S_0$)]}, the former from collisional excitation with the buffer gas and atomic barium in its electronic ground state and the latter from energy pooling accompanying Ba(^3D_J) + Ba(^3D_J) self-annihilation. Measurement of the first-order rate coefficients for the exponential decay of these two emitting states were characterised and where the decay coefficients for the profiles at $\lambda = 791.1$ and 553.5 nm were found to be in the ratio 1:2, respectively, in this long-time regime on the basis of collisional excitation and energy pooling of Ba(^3D_J). The variation of the integrated atomic emission intensities, coupled with optical sensitivity calibrations, are presented for the range of densities of Kr employed. These rate measurements are used to describe quantitatively the collisional and diffusional processes undergone by Ba(^3D_J) with both Kr and with ground state Ba.

Keywords: Ba(^{3}D); Laser excitation; Time-resolved studies; Collisions with Ba; Collisions with Kr; Diffusion

1. Introduction

The low lying states of the electronically excited alkaline earth atoms Mg, Ca and Sr have been the object of extensive investigation by both molecular beams and studies in the time-domain following pulsed dye-laser excitation where they are directly accessible on optical excitation [1–4]. By contrast, whilst the collisional behaviour of the low lying optically metastable states of atomic barium, namely, Ba[6s5d($^3D_{1,2,3}$)] (1.120, 1.143 and 1.190 eV, respectively [5] and Ba[6s5d($^1D_2$)] (1.413 eV [5]) are of considerable interest both in the single-collision condition and the time-domain [1–4], the former is certainly not readily accessible on laser excitation. These states have normally been populated by a range of radiative and collisional processes following initial laser excitation via more strongly allowed transitions to a higher lying state such as Ba[6s6p($^1P_1$)] ($\tau_c = 8.37 \pm 0.38$ ns [6,7]) or Ba[6s6p($^3P_1$)] ($\tau_c = 1.2 \pm 0.1$ μs [8–10]) as described in Part I [11] in the presence of He. In this paper, we present a kinetic investigation of Ba[6s5d(^3D_J)], 1.151 eV above the 6s^2($^1S_0$) ground state in the presence of krypton following the initial pulsed dye-laser excitation of atomic barium vapour at elevated temperature at $\lambda = 553.5$ nm {Ba[6s6p($^1P_1$)] ← Ba[6s^2($^1S_0$)]}. The kinetic behaviour of Ba(^3D_J) in the presence of krypton has not been reported hitherto by any method previously to best of our knowledge. Ba(^3D_J) has been monitored here by the spectroscopic marker transitions at $\lambda = 791.1$ nm {Ba[6s6p($^3P_1$)] → Ba[6s^2($^1S_0$)]} and $\lambda = 553.5$ nm {Ba[6s6p($^1P_1$)] → Ba[6s^2($^1S_0$)]}, the former from collisional excitation with the buffer gas and Ba(6$^1S_0$) and the latter from energy pooling accompanying

* Corresponding author.

1010-6030/97/$17.00
PII S1010-6030(96)04520-0

$Ba(^3D_J) + Ba(^3D_J)$ self-annihilation. A detail kinetic investigation is presented and employed to describe quantitatively the collisional and diffusional processes undergone by $Ba(^3D_J)$ in Kr which are compared with various measurements for the $Ba(^3D_J)$–He system reported previously. Collisional quenching rate data, particularly by Ba itself has been characterised in various investigations [11–14]. Laser-induced fluorescence measurements on $Ba(^3D_J)$ at $\lambda = 611.3$ nm $\{Ba[5d6p(^3P_2)] \leftarrow Ba[6s5d(^3D_1)]\}$ have been employed in order to study the diffusion of $Ba[6s5d(^3D_J)]$ in noble gases [15] but not, in fact, in Kr, which is included in the present study. The present manuscript describes the general approach for obtaining kinetic data using these spectroscopic marker techniques.

2. Experimental details

The general experimental arrangement for time-resolved monitoring of $Ba(^3D_J)$ in the long time-domain at $\lambda = 791.1$ nm $\{Ba[6s6p(^3P_1)] \rightarrow Ba[6s^2(^1S_0)]\}$ and $\lambda = 553.5$ nm $\{Ba[6s6p(^1P_1)] \rightarrow Ba[6s^2(^1S_0)]\}$ has been described previously in Part I [11]. Briefly, $Ba[6s6p(^1P_1)]$ was generated from the pulsed dye-laser excitation of barium vapour [16] in the presence of krypton gas at $\lambda = 553.55$ nm $\{Ba[6s6p(^1P_1)] \leftarrow Ba[6s^2(^1S_0)]\}$. Two monochromator–photomultiplier systems were employed for optical isolation and photoelectric detection of the two atomic emissions employed using small high throughput monochromators. The first, employed for the transition at $\lambda = 553.5$ nm, involved a photomultiplier tube with an S20 response (E.M.I., 9797B) whose gain (G) can sensibly be fitted to the form $\ln(G/\text{arb. units}) = 8.7 \ln(V/V) - 54.4$ [17]. The second employed the new infrared sensitive photomultiplier tube (Hamamatsu R632-S1 response) that we have described previously [18] with a sensitivity range of ca. 400–1200 nm and which was used for the measurements at $\lambda = 791.1$ nm. The gain G of this tube can sensibly be described by the form $\ln G = 8.48 \ln(V/V) - 47.28$ constructed from the commercial gain characteristic. The wavelength response of these two monochromator–photomultiplier systems were calibrated against a quartz–halogen lamp which had previously been calibrated against a spectral radiometer [11]. The forms of the decay profiles themselves are, of course, independent of these calibrations.

As we have stressed hitherto [11], direct emission measurements at $\lambda = 1106.9$ nm $Ba[[6s5d(^3D_1) \rightarrow Ba[6s^2(^1S_0)]$ were not feasible on account of the low sensitivity of the R632-S1 tube in this region, coupled with the relatively low value of A_{nm} for $Ba(^3D_J)$, and hence the spectroscopic marker methods were employed. Whilst emission from $Ba(^1D_2)$ at $\lambda = 877.4$ nm $\{Ba[6s5d(^1D_2)] \rightarrow Ba[6s^2(^1S_0)]$ which is an analogous spectroscopic marker method to that at $\lambda = 791.1$ nm may also monitored using an interference filter in order to improve light collection [11], the emission at $\lambda = 791.1$ nm is much stronger and permits the use of the p.m. tube (Hamamatsu R632)–monochromator combination with the maximum overall response ($\lambda =$ ca. 700 nm [11]) close to this shorter wavelength transition. Hence the $^3P_1$ state resulting from collisional excitation is employed as the marker for $Ba(^3D_J)$ for improved quality in the signals. Decay profiles were captured with a double-channel transient digitiser interfaced to a computer. The materials (Ba (Aldrich Chemicals), Kr (B.O.C. Special Gases)) and other materials used in the laser system were employed essentially as described previously in related studies [11].

3. Results and discussion

Fig. 1 gives examples of the computerised fitting of the digitised output in the long-time domain indicating the first-order decay of the time-resolved atomic emission at $\lambda = 791.1$ nm $(Ba[6s6p(^3P_1)] \rightarrow Ba[6s^2(^1S_0)])$ following the excitation of ground state atomic barium at $\lambda = 553.5$ nm $\{Ba[6s6p(^1P_1)] \leftarrow Ba[6s^2(^1S_0)]\}$ for various elevated temperatures, and hence different concentrations of $Ba[6s^2(^1S_0)]$ in the presence of excess krypton. This relatively strong emission from the $^3P_1$ state $\{\tau_e[Ba6s6p(^3P_1)] = 1.2 \pm 0.1$ μs [8–10]$\}$ in the 'short-time regime' has been considered previously [11]. In the long-time regime, it arises from excitation on energy transfer from the processes of the type (1):

$$Ba[6s5d(^3D_J)] + Ba,Kr \rightarrow Ba[6s6p(^3P_J)] + Ba[6s^2(^1S_0)],Kr \quad \Delta E = +3525\ cm^{-1} \quad (1)$$

At these relatively long times, equilibrium within the spin–orbit components of $Ba(^3D_{1,2,3})$ has been established by col-

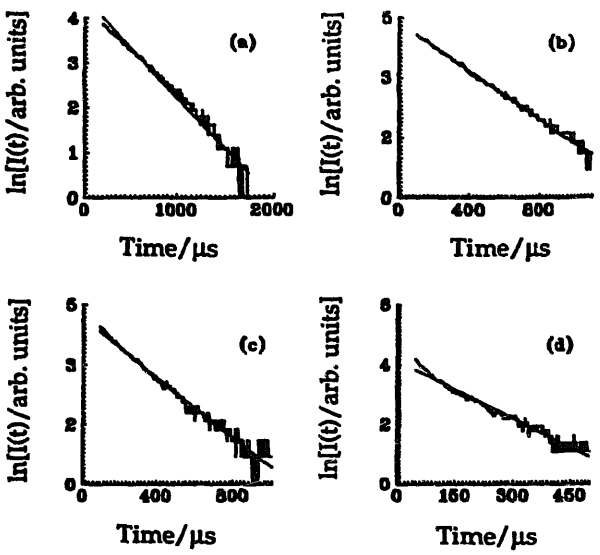

Fig. 1. Examples of the computerised fitting of the digitised output indicating the first-order decay of the time-resolved atomic emission at $\lambda = 791.1$ nm $\{Ba[6s6p(^3P_1)] \rightarrow Ba[6s^2(^1S_0)]\}$ following the pulsed dye-laser excitation of barium atoms at $\lambda = 553.5$ nm $\{Ba[6s6p(^1P_1)] \leftarrow Ba[6s^2(^1S_0)]\}$ in the presence of krypton buffer gas at different temperatures. $p_{Kr} = 30$ Torr.

T/K:	(a) 850	(b) 880	(c) 900	(d) 930
[Ba]/10^{13} atoms cm^{-3}:	(a) 1.7	(b) 3.8	(c) 6.1	(d) 12.3

lisions with the equilibrium density of $Ba(^1S_0)$ [16] at this temperature and $Ba(^3D_J)$ can be considered as a single state.

The first-order decay profiles given in Fig. 1 for the emission at $\lambda = 791.1$ nm $\{Ba[6s6p(^3P_1)] \rightarrow Ba[6s^2(^1S_0)]\}$ indicate exponential decay of the precursor state. It has been shown for the Ba–He system [11] system that this emission acts as a spectroscopic marker for $Ba[6s5d(^3D_J)]$ given that $Ba(6^3P_1)$ results from collisional excitation of this precursor state which follows the exponential decay:

$$Ba[6s5d(^3D_J)]_t = Ba[6s5d(^3D_J)]_{t=0} \exp(-k't) \quad \text{(i)}$$

The first-order decay coefficient for $Ba(^3D_J)$ can thus be written as

$$k' = k'_{cm} + \beta/p_{Kr} + \Sigma k_Q[Q] \quad \text{(ii)}$$

where k'_{cm} will be dominated by electric dipole-allowed emission from $Ba[6s5d(^3D_1)]$ to $Ba[6s^2(^1S_0)]$ in (jj) coupling. Rapid Boltzmann equilibration between the ^3D_J levels will be established in the present system in the long-time regime [19] where we may describe the equilibrium constants connecting these as $^3D_1 \rightleftharpoons {}^3D_2$ ($\Delta\varepsilon = 182\ cm^{-1}$ [5,19]) K_1, and $^3D_2 \rightleftharpoons {}^3D_3$ ($\Delta\varepsilon = 381\ cm^{-1}$ [5,19]) K_2. Assuming emission from this state is then dominated by the electric dipole-allowed transition $^3D_1 \rightarrow {}^1S_0$ (A_{nm}), we may readily show that k'_{cm} is given by

$$k'_{cm} = A_{nm}/(1 + K_1 + K_1K_2) \quad \text{(iii)}$$

where $F = (1 + K_1 + K_1K_2)$ may be readily calculated by statistical thermodynamics.

F takes the value of 3.05 at $T = 800$ K and 3.32 at $T = 1000$ K, reaching a limiting value of 5 at infinite temperature where it is solely determined by the statistical weights within $Ba(^3D_J)$. Decay profiles with various concentrations of Kr at a single temperature were typically carried out at $T = 900$ K where $F = 3.19$. One can immediately see that for measurements across a range of temperature, say 800–1000 K, in order to generate a significant variation in the equilibrium density of $Ba[6s^2(^1S_0)]$, the variation in F is not large and an average value of F at 900 K can be used without serious loss in accuracy. A_{nm} [$= 1/\{\tau_e(^3D_1) = 502\ \mu s\}$] has been characterised recently [20] as $1.99 \times 10^3\ s^{-1}$. The term in β/p_{Kr} describes diffusional loss, which is considered later in more quantitative terms, and $\Sigma k_Q[Q]$, collisional losses of $Ba(^3D_J)$, including excitation to higher states. The emission intensity for states arising from the collisional excitation from $Ba(^3D_J)$ by $Ba(^1S_0)$ and Kr will then take the form:

$$I_{cm}(791.1\ nm) = GS \sum k_E[Kr,Ba]Ba[6s5d(^3D_J)]_{t=0} \exp(-k't) \quad \text{(iv)}$$

where $\Sigma k_E[Kr,Ba]$ represent overall rate coefficients for collisional excitation of $Ba(^3D_J)$ to $Ba(^3P_J)$ in processes (1). G is the gain of the appropriate photomultiplier at the voltage employed and S is the sensitivity of the optical system. All emission intensities can, of course, be normalised to a common relative scale.

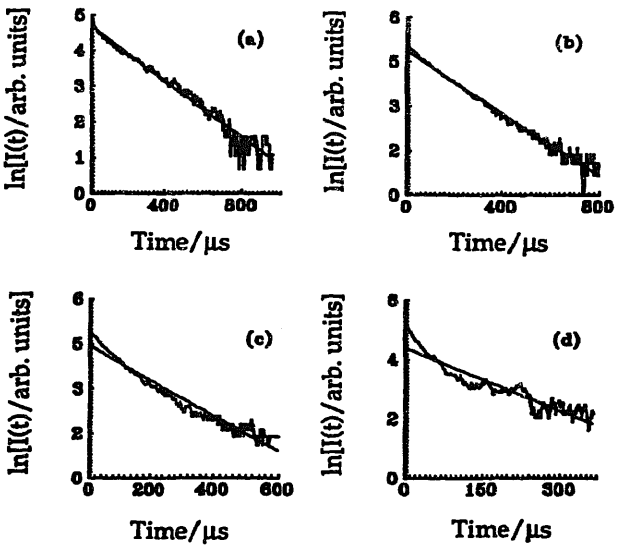

Fig. 2. Examples of the computerised fitting of the digitised output indicating the first-order decay of the time-resolved atomic emission at $\lambda = 553.5$ nm $\{Ba[6s6p(^1P_1)] \rightarrow Ba[6s^2(^1S_0)]\}$ following the pulsed dye-laser excitation of barium atoms at the resonance transition $\{\lambda = 553.5$ nm, $Ba[6s6p(^1P_1)] \leftarrow Ba[6s^2(^1S_0)]\}$ in the presence of krypton buffer gas at different temperatures. $p_{Kr} = 30$ Torr.

T/K:	(a) 850	(b) 880	(c) 900	(d) 930
$[Ba]/10^{13}$ atoms cm^{-3}:	(a) 1.7	(b) 3.8	(c) 6.1	(d) 12.3

Fig. 2 gives examples of first-order decay profiles in the long-time domain for the atomic emission at $\lambda = 553.5$ nm $\{Ba[6s6p(^1P_1)] \rightarrow Ba[6s^2(^1S_0)]\}$ following the resonance excitation of ground state atomic barium at different temperatures in the presence of krypton. $Ba[6s6p(^1P_1)]$ arises from the energy pooling process [5,11]:

$$Ba[6s5d(^3D_J)] + Ba[6s5d(^3D_J)] \rightarrow Ba[6s6p(^1P_1)] + Ba[6s^2(^1S_0)] \quad \Delta E = +654\ cm^{-1} \quad (2)$$

The increase in the first-order decay coefficients with temperature reflects the increasing role of collisional quenching of $Ba(^3D_J)$ by $Ba(^1S_0)$ itself whose density was varied in these studies from 1.7×10^{13} atoms cm^{-3} (850 K) to 12.3×10^{13} atoms cm^{-3} (930 K) [16]. By contrast with the emission intensity at $\lambda = 791.1$ nm, that at $\lambda = 553.5$ nm $\{Ba[6s6p(^1P_1)] \rightarrow Ba[6s^2(^1S_0)]\}$ in the long-time regime following initial excitation at $\lambda = 553.5$ nm and arising from energy pooling between $Ba[6s5d(^3D_J)] + Ba[6s5d(^3D_J)]$ [11,21] (process (1)), and characterised here by a rate constant simply written as $k_{E.P.}$, occurs on a shorter time-scale. Thus, the intensity of the emission at $\lambda = 553.5$ nm arising from this energy pooling will follow the form:

$$I_{cm}(553.5\ nm) = GSk_{E.P.}Ba[6s5d(^3D_J)]^2_{t=0} \exp(-2k't) \quad \text{(v)}$$

where G and S take the appropriate values for the conditions of p.m. voltage and the wavelength employed in this case.

Fig. 3 shows the variation of the first-order rate coefficients for the decay profiles at $\lambda = 791.1$ nm and $\lambda = 553.5$ nm derived from plots of the type given in Figs. 1 and 2 against

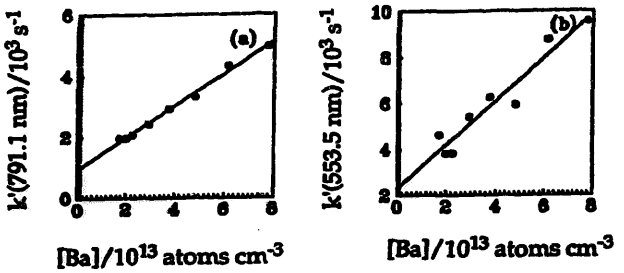

Fig. 3. Variation of the first-order rate coefficients, k', derived from the atomic emission profiles at (a) $\lambda = 791.1$ nm $\{Ba[6s6p(^3P_1)] \rightarrow Ba[6s^2(^1S_0)]\}$ and (b) $\lambda = 553.5$ nm $\{Ba[6s6p(^1P_1)] \rightarrow Ba[6s^2(^1S_0)]\}$ following the pulsed dye-laser excitation of barium atoms at $\lambda = 553.5$ nm $\{Ba[6s6p(^1P_1)] \leftarrow Ba[6s^2(^1S_0)]\}$ in the presence of krypton buffer gas ($p_{Kr} = 30$ Torr) at different concentrations of atomic barium via the use of different temperatures.

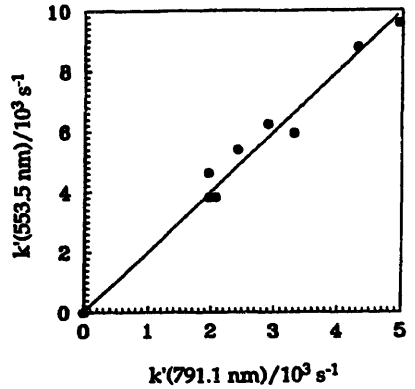

Fig. 4. Comparison of the first-order rate coefficients, k', derived from the emission intensity profiles for the decays at $\lambda = 553.5$ nm $\{Ba[6s6p(^1P_1)] \rightarrow Ba[6s^2(^1S_0)]\}$ and $\lambda = 791.1$ nm $\{Ba[6s6p(^3P_1)] \rightarrow Ba[6s^2(^1S_0)]\}$ following the pulsed dye-laser excitation of barium atoms at $\lambda = 553.5$ nm $\{Ba[6s6p(^1P_1)] \leftarrow Ba[6s^2(^1S_0)]\}$ in the presence of krypton buffer gas ($p_{Kr} = 30$ Torr) at different concentrations of atomic barium via the use of different temperatures (840–920 K).

the concentration of atomic barium. The slopes of these plots yield total quenching rate constants for the removal of $Ba(^3D_J)$ by $Ba(^1S_0)$, the former $k(Ba^3D_J + Ba) = 5.2 \times 10^{-11}$ cm^3 atom^{-1} s^{-1} at the average temperature of $T = 890$ K over which measurements were made, and the latter $2k(Ba^3D_J + Ba) = 9.5 \times 10^{-11}$ cm^3 atom^{-1} s^{-1} ($T = 890$ K) from which we may take the average value of $k(Ba^3D_J + Ba) = (5.0 \pm 0.3) \times 10^{-11}$ cm^3 atom^{-1} s^{-1} ($T = 890$ K). This may be compared with the estimate we have recently reported of $k(Ba^3D_J + Ba$, $T = 900$ K) $\approx 2 \times 10^{-11}$ cm^3 atoms^{-1} s^{-1} from measurements of the type presented in Figs. 1 and 2 [11] with He as the buffer gas and other values, adjusted by the present authors [11] using recent measurements of the vapour pressure of Ba, namely, ($k(Ba^3D_J + Ba)$/cm^3 atom^{-1} s^{-1}: ($T \approx 730$ K), 1.3×10^{-10} [11,12]; (900–1150 K), 3.9×10^{-11} [11,13]; ($T = 850$ K), 5.1×10^{-11} [11,14]). The data in Fig. 3(a) and (b) may also be used to compare the first-order rate coefficients for the decay of $Ba(^1P_1)$, $k'(^1P_1)$ at $\lambda = 553.5$ nm with that of $Ba(^3P_J)$, $k'(^3P_J)$ at $\lambda = 791.1$ nm taken under identical conditions and demonstrating a large variation in the decay coefficients resulting from the density of $Ba(^1S_0)$. This is shown in Fig. 4 whose slope is found to be 2.0 ± 0.2 in accord with Eqs. (iv) and (v).

Fig. 5 gives examples of the digitised output for the decay of the time-resolved atomic emission at $\lambda = 791.1$ nm $\{Ba[6s6p(^3P_1)] \rightarrow Ba[6s^2(^1S_0)]\}$ and $\lambda = 553.5$ nm $\{Ba[6s6p(^1P_1)] \rightarrow Ba[6s^2(^1S_0)]\}$ in the presence of krypton at different pressures at a fixed temperature ($T = 900$ K) with the associated first-order decay profiles given in Fig. 6. The resulting variation of the first-order rate coefficients, $k'(\lambda = 791.1$ nm) and $k'(553.5$ nm) with p_{Kr} are shown in Fig. 7. With such measurements, it is necessary to consider spontaneous emission from $Ba(^3D_1)$, diffusional loss and collisional removal of $Ba(^3D_J)$ by Kr simultaneously. Given rapid Boltzmann equilibration between the ^3D_J levels [19], emission from this state is described by the electric dipole-allowed transition $^3D_1 \rightarrow {}^1S_0$ (A_{nm}) and Eq. (iii). At low pressure, diffusional loss is dominant; at pressures above ca. 10 Torr, diffusional and collisional loss by Kr are in close balance. Thus, we may write

$$k'(791.1\text{ nm}) = A_{nm}(^3D_1)/F + \beta/p_{Kr} + k_{Ba}[Ba] + k_{Kr}p_{Kr} \quad \text{(vi)}$$

and

$$k'(553.5\text{ nm}) = 2A_{nm}(^3D_1)/F + 2\beta/p_{Kr} + 2k_{Ba}[Ba] + 2k_{Kr}p_{Kr} \quad \text{(vii)}$$

where the rate constants for removal of $Ba(^3D_J)$ by Ba (k_{Ba}) and Kr (k_{Kr}) are implicitly presented in a different system of

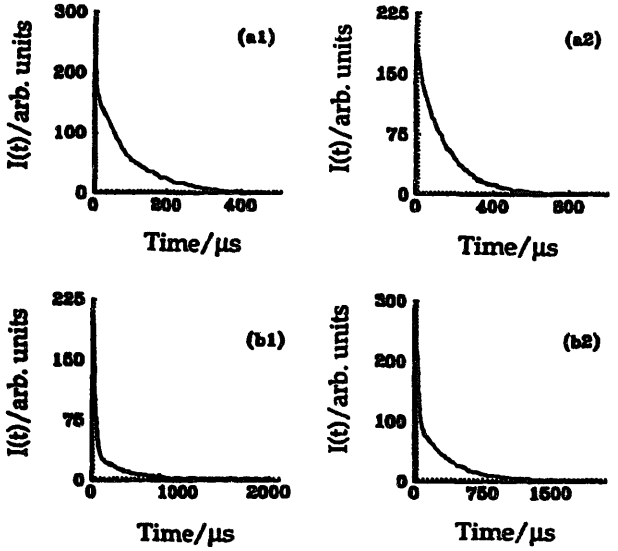

Fig. 5. Examples of the digitised output showing the decay of the time-resolved atomic emission at (a) $\lambda = 553.5$ nm $\{Ba[6s6p(^1P_1)] \rightarrow Ba[6s^2(^1S_0)]\}$ and (b) $\lambda = 791.1$ nm $\{Ba[6s6p(^3P_1)] \rightarrow Ba[6s^2(^1S_0)]\}$ and following the pulsed dye-laser excitation of barium atoms at $\lambda = 553.5$ nm, $Ba[6s6p(^1P_1)] \leftarrow Ba[6s^2(^1S_0)]\}$ in the presence of krypton buffer gas at different pressure ($T = 900$ K).

$\lambda = 553.5$ nm:	p_{Kr}/Torr:	(a1) 3.0	(a2) 30
$\lambda = 791.1$ nm:	p_{Kr}/Torr:	(b1) 3.0	(b2) 30

units on account of the diffusional loss of $Ba(^3D_J)$ being inversely proportional to pressure. The data in Fig. 7(a) and (b) are recast in the forms

$$\{k'(791.1\text{ nm}) - A_{nm}(^3D_1)/F - k_{Ba}[Ba]\}p_{Kr} = \beta + k_{Kr}p_{Kr}^2 \quad \text{(viii)}$$

and

$$\{k'(553.5\text{ nm}) - 2A_{nm}(^3D_1)/F - 2k_{Ba}[Ba]\}p_{Kr} = 2\beta + 2k_{Kr}p_{Kr}^2 \quad \text{(ix)}$$

respectively. Hence we may plot the data for Fig. 7(a) and (b) in the forms of Eqs. (viii) and (ix) and plot $\{k'(791.1\text{ nm}) - A_{nm}(^3D_1)/F - k_{Ba}[Ba]\}[Kr]$ versus $[Kr]^2$ (Fig. 8(a)) and $\{k'(553.5\text{ nm}) - 2A_{nm}(^3D_1)/F - 2k_{Ba}[Ba]\}[Kr]$ versus $[Kr]^2$ (Fig. 8(b)) in order to obtain a value for k_{Kr}. Fig. 8(a) yields $k_{Kr} = 7.6\times10^{-16}$ cm^3 atoms^{-1} s^{-1} and Fig. 8(b), $k_{Kr} = 1.2\times10^{-15}$ cm^3 atoms^{-1} s^{-1} from which we report an average value of $k_{Kr} = (1.0\pm0.3)\times10^{-15}$ cm^3 atoms^{-1} s^{-1} (900 K). The result for k_{Kr} has not been reported hitherto. It may be compared with the result for $k_{Q,He} \approx 1\times10^{-18}$ cm^3 atom^{-1} s^{-1} reported by Whitkop and Wiesenfeld [12] and an estimate of $< 1.6\times10^{-15}$ cm^3 atom^{-1} s^{-1} derived from detailed balance from data for the rate constant for the reverse process of collisional excitation to $Ba(^3P_J)$ ($< 6.6\times10^{-13}$ cm^3 atom^{-1} s^{-1}) reported by Kallenbach and Koch [22,23]. Whilst collisional quenching of $Ba(^3D_J)$ by Kr appears to be marginally more efficient than He, the result still appears to indicate that the main route for collisional loss of $Ba(^3D_J)$ by Kr is excitation to $Ba(^3P_J)$ and not quenching to the ground state with the large accompanying transfer of electronic energy to translation.

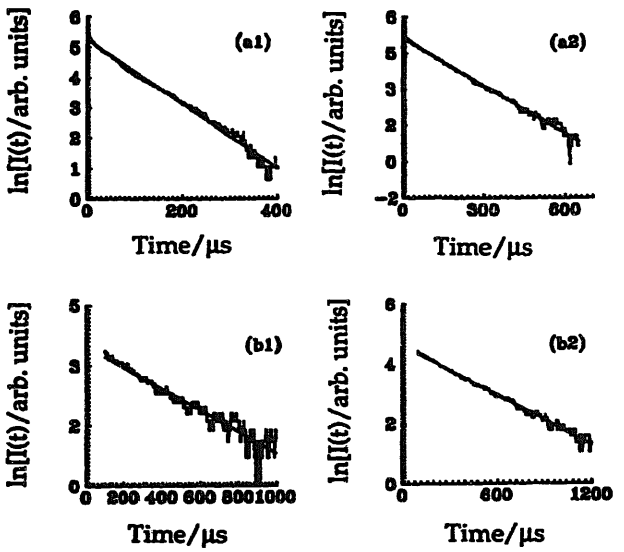

Fig. 6. Examples of the computerised fitting of the digitised output indicating the first-order decay of the time-resolved atomic emission at (a) $\lambda = 553.5$ nm $\{Ba[6s6p(^1P_1)] \rightarrow Ba[6s^2(^1S_0)]\}$ and (b) $\lambda = 791.1$ nm $\{Ba[6s6p(^3P_1)] \rightarrow Ba[6s^2(^1S_0)]\}$ and following the pulsed dye-laser excitation of barium atoms at $\lambda = 553.5$ nm $Ba[6s6p(^1P_1)] \leftarrow Ba[6s^2(^1S_0)]\}$ in the presence of krypton buffer gas at different pressure ($T = 900$ K).

$\lambda = 553.5$ nm: p_{Kr}/Torr: (a1) 3.0 (a2) 30
$\lambda = 791.1$ nm: p_{Kr}/Torr: (b1) 3.0 (b2) 30

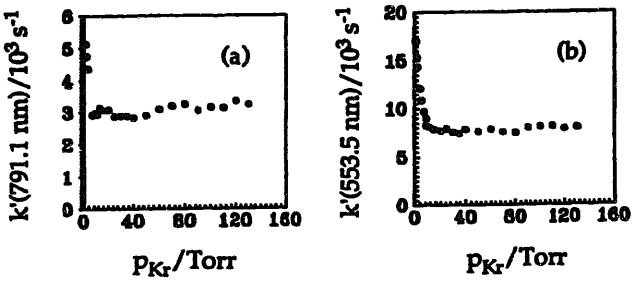

Fig. 7. Variation of the first-order rate coefficients, k' derived from the atomic emission intensity profiles in the long-time domain at (a) $\lambda = 791.1$ nm $\{Ba[6s6p(^3P_1)] \rightarrow Ba[6s^2(^1S_0)]\}$ and (b) $\lambda = 553.5$ nm $\{Ba[6s6p(^1P_1)] \rightarrow Ba[6s^2(^1S_0)]\}$ following the pulsed dye-laser excitation of barium atoms at $\lambda = 553.5$ nm $\{Ba[6s6p(^1P_1)] \leftarrow Ba[6s^2(^1S_0)]\}$ at $T = 900$ K in the presence of varying krypton buffer gas pressure.

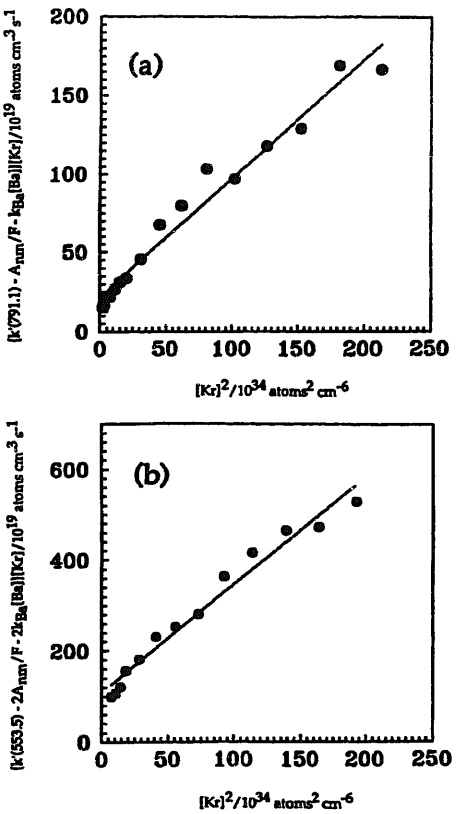

Fig. 8. Variation of the first-order rate coefficients, k' derived from the atomic emission intensity profiles in the long-time domain at (a) $\lambda = 791.1$ nm $\{Ba[6s6p(^3P_1)] \rightarrow Ba[6s^2(^1S_0)]\}$ and (b) $\lambda = 553.5$ nm $\{Ba[6s6p(^1P_1)] \rightarrow Ba[6s^2(^1S_0)]\}$ following the pulsed dye-laser excitation of barium atoms at $\lambda = 553.5$ nm $\{Ba[6s6p(^1P_1)] \leftarrow Ba[6s^2(^1S_0)]\}$ at $T = 900$ K in the presence of varying krypton buffer gas pressure ($F = 1 + K_1 + K_1K_2$). (a) $\lambda = 791.1$ nm: $\{k' - A_{nm}/F - k_{Ba}[Ba]\}[Kr]$ vs. $[Kr]^2$. (b) $\lambda = 553.5$ nm: $\{k' - 2A_{nm}/F - 2k_{Ba}[Ba]\}[Kr]$ vs. $[Kr]^2$.

Eqs. (viii) and (ix) may further be recast in the forms:

$$\{k'(791.1\text{ nm}) - A_{nm}(^3D_1)/F - k_{Ba}[Ba]\}/p_{Kr} = \beta/p_{Kr}^2 + k_{Kr} \quad \text{(x)}$$

and

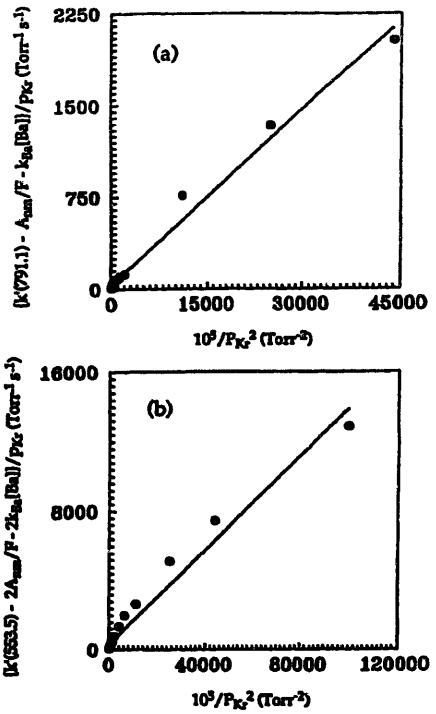

Fig. 9. Variation of the first-order rate coefficients, k' derived from the atomic emission intensity profiles at (a) $\lambda = 791.1$ nm {Ba[6s6p($^3P_1$)] → Ba[6s^2($^1S_0$)]} (b) $\lambda = 553.5$ nm {Ba[6s6p($^1P_1$)] → Ba[6s^2($^1S_0$)]} following the pulsed dye-laser excitation of barium atoms at $\lambda = 553.5$ nm {Ba[6s6p($^1P_1$)] ← Ba[6s^2($^1S_0$)]} at $T = 900$ K in the presence of varying krypton buffer gas pressure presented in the forms ($F = 1 + K_1 + K_1K_2$): (a) $\{k'(791.1) - A_{nm}/F - k_{Ba}[Ba]\}/p_{Kr}$ vs. $1/p_{Kr}^2$ (b) $\{k'(553.5) - 2A_{nm}/F - 2k_{Ba}[Ba]\}/p_{Kr}$ vs. $1/p_{Kr}^2$.

$$\{[k'(553.5\text{ nm}) - 2A_{nm}(^3D_1)/F - 2k_{Ba}[Ba]\}/p_{Kr} = 2\beta/p_{Kr}^2 + 2k_{Kr} \quad \text{(xi)}$$

which are presented in Fig. 9 for the low pressure region where diffusional loss is dominant. The resulting values yield $\beta = 4800$ Torr s^{-1} (Fig. 9(a)) and $\beta = 6750$ Torr s^{-1} (Fig. 9(b)) from which we take the average value of 5800 Torr s^{-1} (900 K). A high accuracy cannot be placed on this value as it results from abstracting from the measured values of k' the large first-order contributions of collisional quenching of Ba(^3D_J) by Kr and, especially, Ba and the effect of spontaneous emission. The forms in the plots in Fig. 9 is in approximate accord with Eq. (x) Eq. (xi). The value of β may be combined with the long-time solution of a diffusion equation of a cylinder [24,25] ($\beta = [\pi^2/l^2 + 5.81/r^2]D_{12}$) using the dimension of the laser beam of diameter ca. 0.5–0.7 cm. Using the standard $T^{1.5}$ dependence for D_{12} from gas kinetic theory, this yields D_{12}(s.t.p.,Kr) = 0.18 cm^2 s^{-1}. Walker et al. [15] have carried out a systematic study of diffusion of Ba(^3D_J) in noble gases, unfortunately, excluding Kr, obtained from laser-induced fluorescence measurements at $\lambda = 611.3$ nm {Ba[5d6p($^3P_2$)] ← Ba[6s5d($^3D_1$)]} following initial laser excitation at $\lambda = 553.5$ nm. These authors [15] report also values of D_{12}(s.t.p.) for Ba(^3D_J) in He, Ne, Ar and Xe of 0.560, 0.201, 0.143 and 0.084 cm^2 s^{-1}, respectively. The present result for D_{12}(s.t.p.,Kr), critically dependent on the geometries employed for laser excitation and light collection, is in approximate accord with the values reported by Walker et al. [15] using their laser induced fluorescence measurements on Ba[6s5d(^3D)–5d6p(^3P)] following modulated excitation at $\lambda = 553.5$ nm.

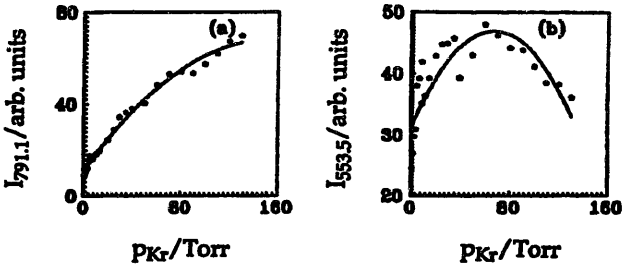

Fig. 10. Variation of the integrated atomic emission intensities at (a) $\lambda = 791.1$ nm {Ba[6s6p($^3P_1$)] → Ba[6s^2($^1S_0$)]} and (b) $\lambda = 553.5$ nm {Ba[6s6p($^1P_1$)] → Ba[6s^2($^1S_0$)]} following the pulsed dye-laser excitation of barium atoms at $\lambda = 553.5$ nm {Ba[6s6p($^1P_1$)] ← Ba[6s^2($^1S_0$)]} at $T = 900$ K in the presence of varying pressure of krypton buffer gas. (a) $I_{791.1}$ vs. p_{Kr}; (b) $I_{553.5}$ vs. p_{Kr}.

Fig. 10(a) shows the variation of the normalised integrated atomic emission intensities for emission from the state resulting from bimolecular collisional excitation involving Ba(^3D_J) + Kr, $I_{791.1}$, with the pressure of Kr and Fig. 10(b), that from the energy pooled state resulting from Ba(^3D_J) + Ba(^3D_J), $I_{553.5}$, with the krypton pressure. They show fundamentally different forms. The monotonic form of Fig. 10(a) demonstrate the effect of pressure broadening in the initial excitation at $\lambda = 553.5$ nm. At 900 K, the Doppler width which dominates the line profile may be calculated as 1.01×10^{-3} nm whereas the laser width is 3.06×10^{-3} nm and hence pressure broadening affects the initial yield of Ba($^1P_1$). Further, the pressure of krypton does affect collisional transfer from Ba($^1P_1$) to Ba($^3P_2$) and then to Ba(^3D_J) (see earlier). Fig. 10(b) for the energy pooled state, Ba($^1P_1$), is much more sensitive to the yield of Ba(^3D_J) following initial excitation to Ba($^1P_1$) as the emission intensity from this state in the long-time regime is proportional to [Ba(^3D_J)]^2. The maximum in Fig. 10(b) is considered to reflect the role of quenching of Ba(^3D_J) by Kr at higher pressure with a lower yield of Ba(^3D_J) available for energy pooling the to the $^1P_1$ state.

Acknowledgements

We thank the Cambridge Overseas Scholarship Trustees for a Research Studentship held by J.L. during the tenure of which this work was carried out. J.L also thanks the O.R.S. for an award. We also thank the E.P.S.R.C. of Great Britain for the initial purchase of the laser system and a Research Studentship held by one of us (S.A.). Finally, we are also indebted to Dr. George Jones of the DRA (Fort Halstead) for encouragement and helpful discussions.

References

[1] D. Husain and G. Roberts, Bimolecular collisions involving electronically excited alkaline earth atoms, Chapter in J.E. Baggott and M.N.R. Ashfold (eds.), *Gas Phase Bimolecular Processes*, Royal Society of Chemistry, London, 1989, Chapter 6, p. 263.

[2] D. Husain, *J. Chem. Soc. Faraday Trans. 2, 85* (1989) 85.

[3] W.H. Breckenridge and H. Umemoto, in K.P. Lawley (ed.), *Dynamics of the Excited State, Adv. Chem. Phys.*, Vol. L, Wiley, London, 1982, Chapter 5, p. 325.

[4] W.H. Breckenridge, in A. Fontijn and M.A.A. Clyne (eds.), *Reactions of Small Transient Species: Kinetics and Energetics*, Academic Press, London, 1983, Chapter 4, p. 157.

[5] C.E. Moore, *Atomic Energy Levels, Natl. Bur. Stand. Ref. Data Ser., Nat. Bur. Stand. Monograph, 35*, Vols. I–III, US Government Printing Office, Washington, DC, 1971.

[6] S. Niggli and M.C.E. Huber, *Phys. Rev. A, 35* (1987) 2908.

[7] P. Hafner and W.H.E. Schwarz, *J. Phys. B., At. Mol. Phys., 11* (1978) 2975.

[8] C.W. Bauschlicher, Jr., R.L. Jaffe, S.R. Langhoff, F.G. Mascarello and H. Partridge, *J. Phys. B., 18* (1985) 2147.

[9] J. Reader, C.H. Corliss, W.L. Wiese and G.A. Martin, *Wavelengths and Transition Probabilities for Atoms and Atomic Ions, Natl. Bur. Stand. Ref. Data Ser., Nat. Bur. Stand. Monograph 68*, US Government Printing Office, Washington, DC, 1980, p. 367.

[10] B.M. Miles and W.L. Wiese, *Critically Evaluated Transition Probabilities for Ba I and II, Natl. Bur. Stand. Technical Note 474*, US Government Printing Office, Washington, DC, 1969.

[11] S. Antrobus, D. Husain and Jie Lei, *J. Photochem. Photobiol. A: Chem., 103* (1997) 1–9.

[12] P.G. Whitkop and J.R. Wiesenfeld, *J. Chem. Phys., 72* (1980) 1297.

[13] J.L. Carlsten, *J. Phys. B., Atom. Mol. Phys., 7* (1974) 1620.

[14] C. Vadla, K. Niemax, V. Horatic and R. Beuc, *Z. Phys. D., 34* (1995) 171.

[15] T.G. Walker, K.D. Bonin and W. Happer, *J. Chem. Phys., 87* (1987) 660.

[16] D.R. Lide and H.P.R. Frederiske (eds.), *CRC Handbook of Physics and Chemistry* CRC Press, Boca Raton, FL, 75th edn., 1994, p. 4-124.

[17] *E.M.I. Catalogue*, E.M.I. Publications, 1979.

[18] S. Antrobus, D. Husain and Jie Lei, *J. Photochem. Photobiol. A: Chem, 90* (1995) 1.

[19] E. Ehrlacher and J. Huennekens, *Phys. Rev. A, 50* (1994) 4786.

[20] S. Antrobus, D. Husain and Jie Lei, in preparation.

[21] J.A. Neuman, A. Gallagher and J. Cooper, *Phys. Rev. A., 50* (1994) 1292.

[22] A. Kallenbach and M. Koch, *J. Phys. B., At. Mol. Phys., 22* (1989) 1691.

[23] A. Kallenbach and M. Koch, *J. Phys. B., At. Mol. Phys., 22* (1989) 1705.

[24] M.W. Zemansky, *Phys. Rev., 34* (1929) 213.

[25] A.C.G. Mitchell and M.W. Zemansky, *Resonance Radiation and Excited Atoms*, Cambridge University Press, Cambrige, 3rd edn., 1961, p. 246.